

Modelling of the Performance of a Solar Electric-Vapor Compression Refrigeration System in Dry Tropical Regions

Armand Noël Ngueche Chedop¹, Noël Djongyang², Zaatri Abdelouahab³

¹Department of Renewable Energies, The Higher Institute of the Sahel, University of Maroua, PO Box 46, Maroua, Cameroon

²Department of Renewable Energies, The Higher Institute of the Sahel, University of Maroua, PO Box 46, Maroua, Cameroon

³Department of Mechanical Engineering, Faculty of Engineering Science, University of Constantine 1; Cité Filali, Bat: F, N° 2, 25000, Constantine, Algeria

Abstract: This paper presents an assessment of a solar electric-vapor compression refrigeration (SE-VCR) system in a dry tropical area. The specific case of the city of Maroua (14.33°E, 10.58°N), located in the Sudano-Sahelian climatic region of Cameroon is considered. The overall evaluation of the hourly cooling loads and the performance of the system were done by the means of heat balance method. The results showed that, for an evaporating temperature of 0 °C, the effective power of the compressor varies between 5.33 kW and 6 kW, the capacity of the condenser varies between 24 and 28 kW, and the coefficient of performance varies from 3.28 to 3.74 while the efficiency of the installation varies between 17 % and 35 %. Regulations on new installations of air-conditioners require COP values of at least 3, so SE-VCR system could successfully be operated in dry tropical areas to improve thermal comfort in living environments.

Keywords: Solar refrigeration, SE-VCR system, Thermal comfort, Dry tropical regions.

1. Introduction

During the last decades, particularly high temperatures during scorching heat seasons due to climate change, have led to a rapid development of air conditioning in the habitat. The development of air conditioning related to the improvement of living conditions, leads to increased energy consumption in the habitat. Globally, the production of cold in habitat appears to be a major energy challenge. In fact, the first station of the specific electricity consumption (excluding heating) of housing is the production of domestic cold. It represents a third of the worldwide energy consumption (approximately 1000 kWh/year) [1,2]. According to Djongyang *et al.* [2], the economic growth of developing countries will surely involve a growing need for cold. In the current energy crisis, solar energy can be an efficient solution [3]. Indeed, this heat energy at moderate temperatures is available everywhere in an intermittent form, particularly in Africa where it is an inexhaustible source. So far, it has been really used in the field of water heating, drying processes and photovoltaic conversion [3]. Solar energy applications in different fields have been increasing gradually. Several studies showed that, cold production from this energy is possible [2]. In fact, PV system is the most appropriate system for small capacity refrigeration plants used for food or medical applications in areas far from conventional energy sources, where a high level of solar radiation is present [4,5]. Solar cooling can be broadly categorized into solar electric refrigeration, solar thermal refrigeration and solar thermal air-conditioning [6]. In the first category, the solar electric compression refrigeration uses photovoltaic (PV) panels to power conventional refrigeration machine. In the second category, the refrigeration effect can be produced through solar thermal gain. Here, the solar mechanical compression refrigeration, solar absorption refrigeration and solar

adsorption refrigeration are the three common options. In the third category, the conditioned air can be directly provided through the solar thermal gain by means of desiccant cooling [7].

The attractiveness of “free” cooling obtained from the sun has spawned a wealth of research over the last several decades, as summarized in a number of review articles [8]. Most review articles were limited to solar thermal refrigeration technologies [9-13]. However, several studies including different technologies of solar cooling are found in the literature. Xu *et al.* [14] investigated on solar powered absorption refrigeration (SPAR) system with advanced energy storage technology. Their study paves the road for system design and operation control in the future. Some models to evaluate the interest of the technique depending on climatic conditions and types of construction also exist. Fong *et al.* [15] studied a solar hybrid air-conditioning system using adsorption refrigeration, chilled ceilings and desiccant dehumidification. They found that the proposed solar hybrid air-conditioning system is technically feasible through high temperature cooling. They concluded that, among the three types of chilled ceilings, the passive chilled beam is the most energy-efficient option to work with the solar adsorption refrigeration for space conditioning in subtropical regions. Kaplanis and Papanatasiou [11] described the design and development stages to convert a conventional refrigerator to a solar powered one. Axaopoulos and Theodoridis [16] experimentally investigated a solar photovoltaic powered ice-maker which operates without the use of batteries. It was reported that their study results have shown very good ice-making capability and reliable operation, as well as a great improvement in the startup characteristics of the compressors, which remain operational even during days with low solar irradiation and operate with improved

utilization of the available photovoltaic power. Ewert *et al.* [17] experimentally investigated three different refrigeration technologies (thermoelectric, Stirling, and vapor compression). They reported that proper sizing of solar-refrigerator components and system integration are essential for good design options. Papadopoulos *et al.* [18] focused on the state of the art of thermal solar systems use and on the possibilities of combining those with state of the art technologies in sorption refrigeration, in order to cover the cooling demand of residential and commercial buildings. Sözen and Özalp [19] investigated the usage possibility of solar-driven ejector-absorption cooling systems in Turkey. They reported that it is sufficient to have a collector surface-area of 4 m² with high-performance refrigeration all over Turkey. Desideri *et al.* [20] analyzed the technical and economic feasibility of solar absorption cooling systems, designed for two different application fields (industrial refrigeration and air conditioning). They described different technical installations for solar cooling, their way of operation, advantages and limits. Sanjuan *et al.* [21] developed a full dynamic simulation model that includes the solar collector field, the absorption heat pump system and the building load calculation. It has been applied to optimize the coupling of a system based on this new technology of solar powered absorption heat pump, to a bioclimatic building. It has been shown how strong the influence of the control strategies in the overall performance is, and the importance of using hourly simulations models when looking for highly efficient buildings. Thermo electric methods are also investigated [22,23].

However, most of the studies performed in solar technology field are based on the vapor compression cycle. In fact, among the various systems used, the vapor compression machine coupled with solar panels seems to be very promising in housing air conditioning [24]. The biggest advantage of using solar panels for cooling would be their simple construction and high overall efficiency when combined with a conventional vapor compression system because of its commonly higher coefficient of performance which is more than 1. Mehmet Bilgili [6] investigated on the possibility of improving thermal comfort in the habitat in Adana city, Turkey from solar electric-vapor compression refrigeration (SE-VCR) for different evaporating temperatures. He showed that the SE-VCR system could be used efficiently for home/office-cooling purposes during the day in the southern region of Turkey.

Today, decrease in the cost of PV panels with the increasing PV panel demand, and in parallel to this situation, increase in duration of use (lifetime) of PV panels, use of these systems has been increasing [25], particularly in developing countries. The Sudano-Sahelian region of Cameroon has a great sunning potential (5.71 kWh/m²/day) [3]. Indeed, in the hot period, the demand of energy increases sharply due to heavy use of air conditioning systems. Moreover, researches on the assessment of the hourly performance of SE-VCR systems in dry tropical regions are inexistent. The aim of the present study is to investigate the performance of vapor compression refrigeration powered by solar energy system in Maroua, a typical Sudano-Sahelian city of Cameroon. First, the hourly cooling load capacities (heat gain) of a sample

building during the 1st days of the months from April to October were determined by using meteorological data such as hourly average solar radiations and atmospheric temperatures. Then, the variations of various parameters such as coefficient of the performance, condenser capacity and compressor power consumption during the day were calculated for different evaporating temperatures. In addition, the minimum photovoltaic panel surface area was determined to meet the compressor power demand according to the hourly average solar radiation data. After determining the necessary photovoltaic panel surface area, the solar radiation production on panel surface area and PV power production were obtained.

2. Study Area

Cameroon is situated between latitude of 2°N to 13°N, longitude of 9°E to 17°E and covers a land area of about 475 442 km² (figure 1). An equatorial climate with four seasons (two dry and two rainy) is found in the southern part and Atlantic Ocean coasts with approximately 3 890 mm of precipitation per year. Abundant rainfall occurs from April to November, and practically throughout the year in the southwest mountains (approximately 10 000 mm per year). Three main climatic regions are found: the southern equatorial region, which extends from 2°N to nearly as far as latitude 6°N; the Sudanese region, wet and tropical, extending from 7°N to a little beyond 10°N; the Sudano-Sahelian region (10-13)°N, dry and tropical. The mean outdoor temperatures vary between 25°C in the south, 21.1°C in the central plateau and 32.2°C in the north [26].

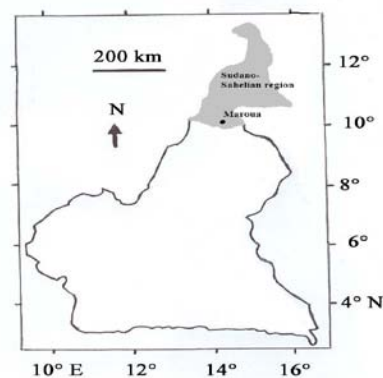


Figure 1: Study area

The current study was carried-out in Maroua (14.33°E, 10.58°N), situated at an altitude of 394 m above sea level. The average temperature is 27.7 °C, while the average insolation is 5.70 kWh/m²/day. The wind speeds are up to 3.8 m/s on average, with peaks around 4.6 m/s. Table 1 presents the monthly average insolation in Maroua (from 2000 to 2010; approximately a solar cycle), while table 2 shows the evolution of the mean monthly outdoor temperatures recorded during the study period.

Table 1: Mean monthly insolation in Maroua from 2000 to 2010 (Source: Meteorological Service of the Airport of Maroua-Salak)

Months	Jan	Feb	Mar	Apr	May	Jun	Jul	Aug	Sep	Oct	Nov	Dec
Insolation	5.61	6.24	6.56	6.31	5.96	5.50	5.03	4.85	5.34	5.70	5.85	5.56

Table 2: Mean hourly variation of outdoor temperature from March to October 2012 in Maroua (Source: Meteorological Service of the Airport of Maroua-Salak)

Time	Months							
	Mar	Apr	May	Jun	Jul	Aug	Sept	Oct
0	29.0	33.2	28.6	28.8	23.4	24.9	25.2	26.5
3	27.0	31.8	25.0	27.5	23.8	23.5	24.5	26.4
6	25.0	32.4	27.2	26.2	23.9	22.8	24.0	25.8
7	26.0	34.3	28.0	26.9	24.0	24.1	25.0	28.4
8	28.7	35.9	34.3	28.6	24.5	25.2	26.8	29.3
9	29.5	38.3	36.7	30.8	26.8	27.7	28.2	31.8
10	31.2	40.6	38.8	31.1	28.7	29.1	29.0	32.5
11	33.0	41.7	40.2	30.7	28.9	30.1	29.2	33.6
12	36.0	42.3	41.2	30.7	29.6	30.7	29.1	33.7
13	37.5	42.3	41.8	31.7	30.3	31.1	29.3	34.0
14	38.0	42.2	41.4	32.4	30.4	31.1	28.9	34.3
15	38.3	41.2	40.0	30.8	30.4	30.6	28.9	33.8
16	37.8	41.8	39.0	25.8	28.0	27.7	26.0	33.0
17	36.0	41.8	37.0	26.2	26.0	25.0	25.0	32.5
18	34.0	37.0	34	26.2	24.0	23.0	24.0	31.7
21	28.3	33.2	30.6	25.5	23	21.8	22.0	29.6
Average	32.2	38.1	35.2	28.7	26.6	26.8	26.6	31.1

From the above it could be seen that the Sudano-Sahelian region of Cameroon is particularly favorable to solar refrigeration system coupled to the photovoltaic.

3. Material and Methods

Figure 2 shows the layout of the sample building studied. It represents the administrative services of the Higher Institute of the Sahel, University of Maroua. (L₁) is the hall, (L₂) the office of the Deputy Director, (L₃) that of the Head of Department of Textile, while (L₄) is the office of the Head of Department of Environmental Sciences.

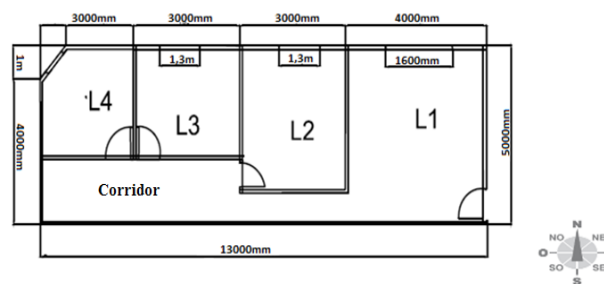


Figure 2: Layout of the studied building

The set-up of the experimental system is presented in figure 3. It includes a motor, a compressor, an evaporator, a condenser, an expansion valve, a battery, an inverter, a PV controller and photovoltaic panels. The SE-VCR system utilizes a solar-powered prime mover to drive a conventional air-conditioning system. This can be done by converting solar energy into electricity by means of photovoltaic

devices, then utilizing an electric motor to drive a vapor compressor.

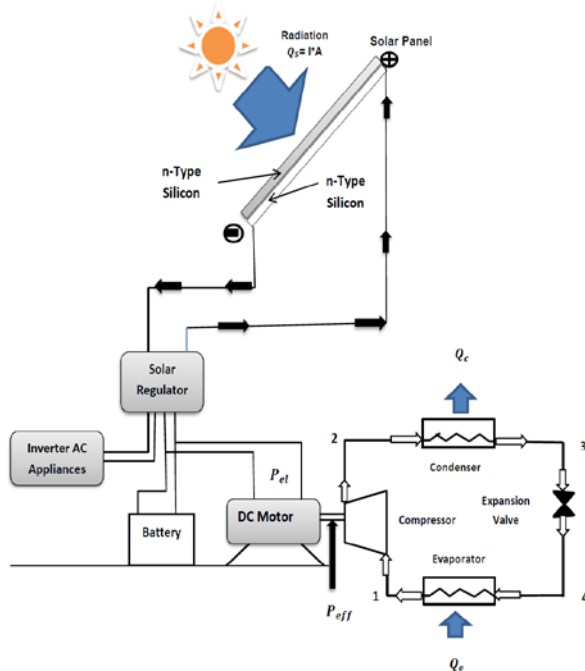


Figure 3: Set-up of the experimental SE-VCR system studied

The thermal fluid (refrigerant) overcomes the cycle presented in figure 4.

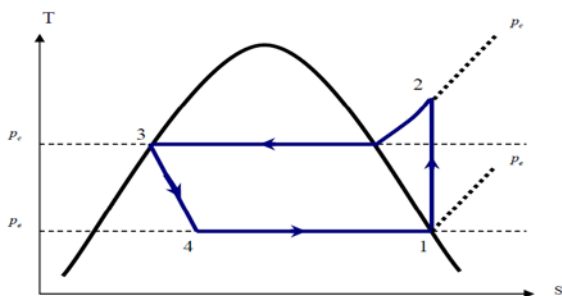


Figure 4: Diagram of vapor-compression thermodynamic cycle (T, S) [34]

3.1 Analysis of the refrigeration system

The compressor power consumption is obtained from the formula [27]:

$$\dot{Q}_{cp} = \dot{m}(h_{2r} - h_1) = \frac{\dot{m}(h_{2is} - h_1)}{\eta_{is}} \quad (1)$$

While the effective compressor power consumption is given by [27]:

$$\dot{Q}_{eff} = \frac{\dot{Q}_{cp}}{\eta_M} = \frac{\dot{m}(h_{2is} - h_1)}{\eta_{is} \cdot \eta_M} \quad (2)$$

where h_i is the specific enthalpy at state i , η_{is} and η_M are respectively the isentropic and the mechanical efficiencies of the compressor, and \dot{m} the mass flow rate of the refrigerant. The indexes r and is are respectively for reversible and isentropic transformations.

The condenser capacity is obtained from [27]:

$$\dot{Q}_{con} = \dot{m}(h_{2r} - h_3) \quad (3)$$

The isentropic efficiency is given by [27,28]:

$$\eta_{is} = \frac{(h_{2is} - h_1)}{(h_{2r} - h_1)} \quad (4)$$

The power transfer at the evaporator is given by [28, 29]:

$$\dot{Q}_{ev} = \dot{m}(h_1 - h_4) \quad (5)$$

The process of expansion valve is assumed to be a throttling process [28], so:

$$h_4 = h_3 \quad (6)$$

h_4 and h_3 represent respectively the specific enthalpies of inlet and outlet valve fluids.

The power balance of the cycle can be written as follows [29]:

$$\dot{Q}_{con} = \dot{Q}_{ev} + \dot{Q}_{eff} \quad (7)$$

The mass flows of liquid refrigerant and volumetric efficiency of the machine are respectively given by [27-29]:

$$\dot{m} = \frac{\dot{V}_b}{V_1} \eta_v \text{ and } \eta_v = \frac{\dot{V}_a}{\dot{V}_b} \quad (8)$$

$$\text{With } \dot{V}_b = \frac{\pi D^2 n N C}{4 \times 60} \text{ and } \dot{V}_a = \dot{m} \cdot V_1 \quad (9)$$

Where \dot{V}_a and \dot{V}_b are respectively the volumetric rates aspired and generated by the compressor; V_1 is the volumetric mass; n the number of piston; N the rotational speed; C the distance travelled by piston, and D the diameter of the piston.

• Coefficient of performance of the refrigeration cycle.

It is obtained from [30]:

$$COP_F = \frac{\dot{Q}_{ev}}{\dot{Q}_{eff}} = \frac{(h_1 - h_4)}{(h_{2is} - h_1)} \eta_{eff} \quad (10)$$

• Efficiency of the refrigeration cycle.

The efficiency of the refrigeration cycle is given by [27]:

$$\eta_f = COP_F \left(\frac{\theta_c - \theta_0}{\theta_0} \right) = \frac{(h_1 - h_4)}{(h_{2is} - h_1)} \eta_{eff} \left(\frac{\theta_c - \theta_0}{\theta_0} \right) \quad (11)$$

Where θ_0 and θ_c are respectively the evaporating and condensing temperatures of the refrigerant.

• Coefficient of the performance of the calorific cycle.

It is given by [30]:

$$COP_C = \frac{\dot{Q}_{con}}{\dot{Q}_{eff}} = \frac{(h_{2r} - h_3)}{(h_{2is} - h_1)} \eta_{eff} \quad (12)$$

• Efficiency of the calorific cycle.

It is given by [30]:

$$\eta_c = COP_C \left(\frac{\theta_c - \theta_0}{\theta_0} \right) = \frac{(h_{2r} - h_3)}{(h_{2is} - h_1)} \eta_{eff} \left(\frac{\theta_c - \theta_0}{\theta_0} \right) \quad (13)$$

3.2 Analysis of various heat inputs

• Heat transmission through the facades (walls, roof, ceiling and floor) and glazing

Heat transmission through the facades and glazing can be

obtained through the formula [31]:

$$Q_{str} = k.S.\Delta\theta \quad (14)$$

k is the thermal transmittance of the wall or glazing in $W/m^2.\text{°C}$, S the surface of the wall or window (m^2), and $\Delta\theta$ the temperature difference between the two faces of the wall (°C).

• **Heat input by solar radiation through the facade**

The radiative heat transfer through the wall can be obtained by [32]:

$$Q_{strm} = \alpha.F.S.R_m \quad (15)$$

where α is the absorption coefficient of the wall receiving the radiation; S the walls' surface (m^2); F the factor of solar radiation, R_m the solar radiation absorbed on the walls' surfaces (W/m^2).

• **Heat input by radiation on the glazing**

The amount of heat passing through the glazing (Q_v) is given by [31]:

$$Q_{svv} = \alpha.g.S.R_v \quad (16)$$

where α is the absorption coefficient of the glazing; g the reduction factor depending on the type of window's protection against solar radiation; S is glass surfaces (m^2), and R_v the intensity of solar radiation on windows (in W/m^2), defined in the same way like R_m .

• **Heat input by air renewal and infiltration**

There are two kinds of heat input by air renewal and infiltration.

- The sensitive gains by air renewal given by [31, 32]:

$$Q_{Sr} = q_v.(\theta_e - \theta_i) \times 0.33 \quad (17)$$

- The latent gains by air renewal obtained from [31]:

$$Q_{Lv} = q_v.(\omega_e - \omega_i) \times 0.84 \quad (18)$$

where q_v is the outdoor airflow renewal (m^3/h), θ_e and θ_i are respectively the basic outdoor and indoor temperatures; ω_e and ω_i are respectively the water contents of the outdoor and indoor air in g per kg of dry air.

In the case of natural ventilation, it can be considered that the air exchange is equal to the room volume per hour ($1vol/h$).

• **Heat input by occupants**

There are two kinds of heat gains generated by the occupants:

- Sensitive gains given by [31]:

$$Q_{Soc} = n.C_{Soc} \quad (19)$$

- Latent gains obtained from the formula [31]:

$$Q_{Loc} = n.C_{Loc} \quad (20)$$

where n is the number of occupants; C_{Soc} the sensitive heat of the occupants (W) and C_{Loc} the latent heat of occupants (W).

• **Heat input by lighting**

The heat input by lighting is a source of sensitive heat and depends on the type of fluorescent lamp. It is evaluated from the following formula:

$$Q_{Secl} = 1.25 P \quad (21)$$

For an incandescent lamp:

$$Q_{Secl} = P \quad (22)$$

with P the lamp power (W). In the case of the fluorescent lamp, 25% of the heat is additional heat generated by the electromagnetic ballast.

• **Heat input by machinery and equipment**

Most devices are both source of sensitive and latent heat. The heat input by machinery and equipment (Q_{Sequip}) are determined from the data provided by the manufacturers. The input of these machines and equipment should be multiply by a coefficient according to their operating times. For example,

a device working a half-hour releases half of its electrical power heat input.

• **Total heat loads**

The total heat balance (Q_T) is the sum of all internal and external loads. It is more convenient to sum sensitive loads (Q_S) and latent loads (Q_L) [31]:

$$Q_T = Q_S + Q_L \quad (23)$$

• **Total sensitive loads**

These are the contributions of sensitive heat in the room, due to the difference between indoor and outdoor temperatures [27]:

$$Q_S = Q_{St} + Q_{Strm} + Q_{Srv} + Q_{Sr} + Q_{Soc} + Q_{Secl} + Q_{Sequip} \quad (24)$$

• **Total latent loads**

These are the contributions of latent heat due to the difference in the amount of indoor and outdoor water vapor [33,34]:

$$Q_L = Q_{Lr} + Q_{Loc} + Q_{Lequip} \quad (25)$$

3.2. Analysis of the solar photovoltaic system

The daily solar energy production is given by [6]:

$$\text{Daily energy production} = \frac{\text{Energy needs}}{\text{Duration of charge / discharge}} \quad (26)$$

The peak power to be installed is obtained from [30]:

$$\text{Peak power} = \frac{\text{Daily energy production}}{\text{Insolation} \times \text{corrective coefficient}} \quad (27)$$

The capacity C of the batteries is obtained from [32]:

$$C = \frac{\text{Daily energy production} \times \text{number of days of autonomy}}{\text{nominal voltage of the battery} \times \text{efficiency} \times \text{depth of discharge} \times \text{corrective factor}} \quad (28)$$

The power of photovoltaic panels P_{pv} is given by the following expression [31]:

$$P_{pv} = \frac{\dot{m}(h_{2i} - h_1) \times 24}{R_{pv} \times R_{acc} \times R_{reg} \times \eta_M \times \eta_{is} \times \eta_{im} \times \eta_{Mel} \times \text{Insolation}} \quad (29)$$

But

$$COP_F = \frac{\phi_F}{P_{eff}} \quad \text{hence}$$

$$P_{pv} = \frac{\phi_F \times 24}{R_{pv} \times R_{acc} \times R_{reg} \times COP_F \times \text{Insolation}} \quad \text{where } \phi_F \text{ is the}$$

refrigerating power; COP_F is the coefficient of the refrigeration performance, R_{ond} is the efficiency of the inverter, R_{acc} the efficiency of the battery, and R_{reg} the efficiency of PV controller.

The global efficiency of the installation η_{inst} is therefore [31]:

$$\eta_{inst} = \frac{R_{pv} \times R_{acc} \times R_{reg} \times COP_F \times \text{Insolation}}{24} \quad (30)$$

4. Results and Discussion

4.1 Balance of thermal loads

The various heat transfers through the environment are given in tables 3-5. For the equipments, we have three refrigerators, two photocopiers, four desktops computers, eight laptops, three coffee pots, four inverters and three printers. The coefficient of use (cu) of each device has been considered while a mean value of 13 persons is used.

Table 3: Walls, floor, ceilings, panes, and doors heat contributions in the building

Walls' orientation	Surface (m ²)	k (W/m ² .K)	Intensity of the radiation (W/m ²)
Northern wall	52	2.09	280
Western wall	20	2.09	359
Floor	65	1.36	-
Ceiling	65	1.14	-
Northern Panes	13	6	224
Northern Doors	2	3.94	284

Table 4: Heat exchanges by transmission and radiation through the walls

Walls' orientation	North	West	East	South	Northern pane	Ceiling	Wooden doors	Northern doors	Total
Transmission thermal loads (W)	760.76	292.60	862.60	331.80	546.00	518.70	165.48	-	3478.02
Radiative thermal loads (W)	611.52	301.56	-	-	701.20	518.7	-	78.33	1692.62

Table 5: Heat exchanges by occupants, equipment and air renewal through natural ventilation

Thermal loads	Sensitive heat Q _s (W)	Latent heat Q _L (W)	Total (W)
Air renewal (1)	415.80	257.04	672.84
Occupants (2)	65.52	70.20	135.72
Equipment (3)	7740.10	225,00	7965.1

Assuming a coefficient of security of 5%, the global heat balance will therefore be equal to $Q_T = 1.05 * Q_t = 22\ 202\ W$. The total heat balance varies with time as shown in figure 5.

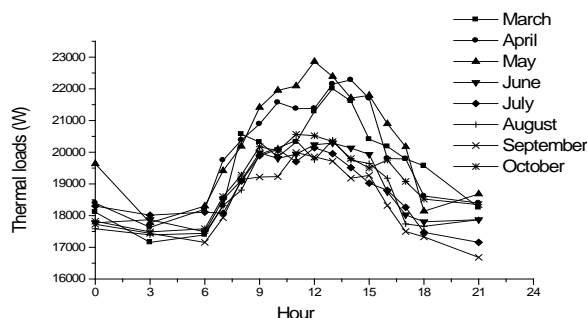


Figure 5: Hourly variation of the thermal loads in the building for the 1st days of the months from March to October 2012, for an evaporating temperature Te= 0°C

It could be seen that the maximum load occurs in May around 1 pm with a value of 22.89 kW while the minimum occurs around 3 am with a value of 17.63 kW. From June to September, the thermal loads are low and vary less compared to each other. This can be explained by the decrease in insolation during that period. Generally, the thermal loads are higher between 9 am and 3 pm and lower between 4pm and 7 am. It could also be seen that the periods of high thermal loads correspond to periods of high activities in the building; consequently the necessity of low temperature is needed.

4.2 Computation of the compressor power consumption

Table 6 presents the values of compressor power consumption for an evaporating temperature of 0 °C and condensing temperature of 40 °C on the 1st day of the months from March to October 2012 at 1 am ($h_{2is}=425\ kJ/kg; h_4=250\ kJ/kg; h_1=395\ kJ/kg$ and $\dot{m}=0.153\ kg/s$).

Table 6: Monthly variation of the effective power of the compressor

Months	Mar	Apr	May	Jun	Jul	Aug	Sep	Oct
Effective power (kW)	5.95	6.00	5.99	5.48	5.39	5.51	5.33	5.5

Figure 6 shows the hourly evolution of the compressor power consumption on the 1st day of the month from March to October 2012. The maximum values are also obtained between 9 am and 3 pm, with a peak in the month of May (6.18 kW at 12 pm), while they are lowest between 4 pm and 7 am, with a minimum value of 4.51 kW in September at 9 pm. It could be easily checked that, there is a close relationship between thermal loads and compressor power consumption. In fact, the compressor needs more energy to fulfill the needs of cooling in the building.

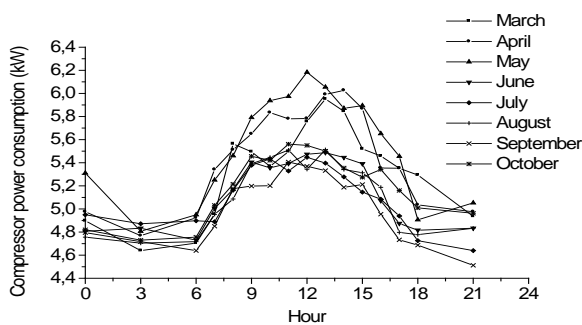


Figure 6: Hourly variation of the compressor power consumption for the 1st days of the months from March to October 2012, for an evaporating temperature $T_e = 0^\circ\text{C}$.

Figure 7 shows the variation of the hourly compressor power consumption for the evaporating temperatures of -10°C , -5°C , 0°C , 5°C and 10°C . It could be seen that this power decreases with increasing evaporating temperatures. For

$T_e = -10^\circ\text{C}$, the compressor power consumption values varies between 2.90 kW at 3 am and 3.73 kW at 12 am, while for $T_e = -10^\circ\text{C}$ we have powers ranging from 5.84 kW to 7.36 kW.

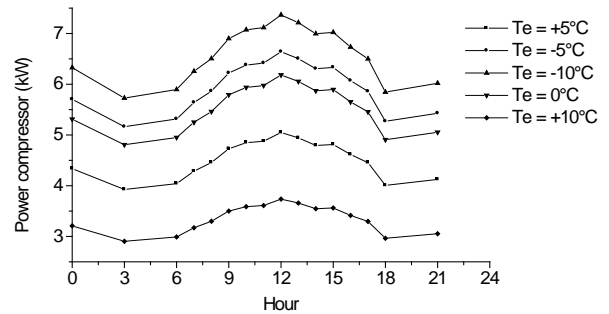


Figure 7: Hourly variation of the compressor power consumption for the evaporating temperatures of 0°C , $+10^\circ\text{C}$, $+5^\circ\text{C}$, -5°C and -10°C in April 1st, 2012.

4.3. Computation of the coefficient of the performance COP_F

Table 7 presents the values of the COP_F for an evaporating temperature of 0°C and condensing temperature of 40°C for the 1st days of the months from March to October 2012 at 1 am. It could be seen that the COP_F varies with time as shown in figure 8.

Table 7: Monthly variation of the coefficient of the performance

Months	Mar	April	May	Jun	Jul	Aug	Sep	Oct
COP_F	3.66	3.74	3.69	3.73	3.38	3.32	3.28	3.38

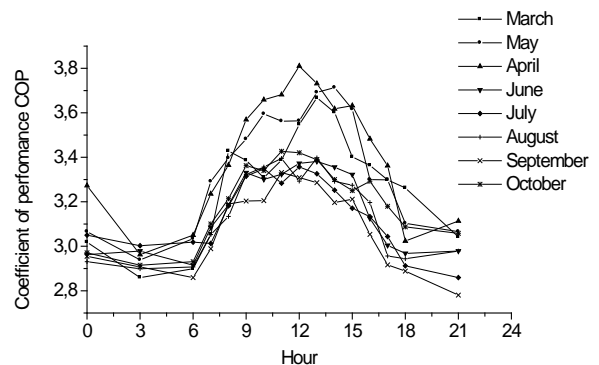


Figure 8: Hourly variation of the coefficient of the performance for the 1st days of the months from March to October 2012, for an evaporating temperature $T_e = 0^\circ\text{C}$

This coefficient was calculated by evaluating the temperatures and thermal loads at different hours of the day. It could be seen that the COP_F is lower at 3 am with values between 2.90 and 2.96. This can be explained by the fact that, at that hour of the day, the heat load decreases significantly in the building but also by the absence of occupants. The highest values are obtained from 12 am and 1 pm with values between 3.73 and 3.81. The peak is obtained in April around 1 pm where we have an outdoor temperature of $43^\circ C$. Regulations on new installations of air-conditioners require COP values of at least 3 [8]; SE-VCR system could successfully be operated in dry tropical areas to improve thermal comfort in living environments.

Figure 9 shows the variation of the COP_F with the evaporating temperature. It could be seen that, the evaporating temperature of the system, significantly influences the coefficient of performance. For an evaporating temperature of $0^\circ C$, the coefficient of performance varies from 2.9 to 3.8 while it is slightly higher for an evaporating temperature of $10^\circ C$ where it reaches its maximum at 6.58. Conversely, for the lower evaporating temperature of $-10^\circ C$, the COP_F ranges from 2.52 to 3.18.

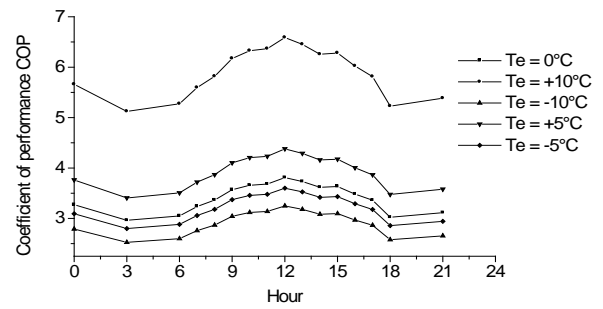


Figure 9: Hourly variation of the coefficient of the performance for evaporating temperatures of $0^\circ C$, $+10^\circ C$, $+5^\circ C$, $-5^\circ C$ and $-10^\circ C$ on April 1st, 2012

4.4. Evaluation of the capacity of the condenser

For an evaporating temperature of $0^\circ C$ and condensing temperature of $40^\circ C$, the values of the capacity of the condenser are obtained as shown in Table 8 for the 1st days of the months from March to October 2012 at 1 pm ($h_{2r} = 430$ kJ/kg; $h_3 = 250$ kJ/kg; $h_1 = 395$ kJ/kg and $\dot{m} = 0.153$ kg/s). The heat output of the condenser is also function of the local heat load and the evaporating temperature as shown in figure 10.

Table 8: Monthly variation of the capacity of the condenser

Months	Mar	Apr	May	Jun	Jul	Aug	Sep	Oct
P_c (kW)	27.31	27.79	27.49	25.18	24.77	25.30	24.47	25.24

It could be seen that the capacity of the condenser increases with evaporating temperatures.

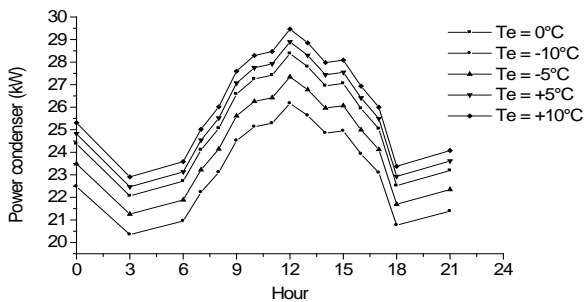


Figure 10: Hourly variation of the capacity of the condenser for the evaporating temperatures of $0^\circ C$, $+10^\circ C$, $+5^\circ C$, $-5^\circ C$ and $-10^\circ C$ in April 1st, 2012.

Figure 11 shows the evolution of the heat output of the condenser for different times of the 1st days of the months from March to October 2012. It could be seen that the maximum power was obtained in April at 1 pm with a value of 28.37 kW, while the minimum was obtained in September at 9 pm with a substantial value of 20.70 kW. Here again, one can see that the heat output depends on the condenser temperature and also on occupants.

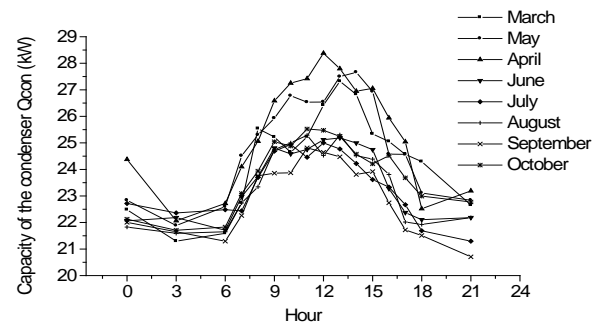


Figure 11: Hourly variation of the capacity of the condenser for 1st days of the months from March to October 2012, for an evaporating temperature $Te = 0^\circ C$.

4.5. Power of the Solar Modules

For a continuous use, a corrective coefficient of 0.73 and monocrystalline silicon technology with a peak power of 220 Wp and 24V power voltage were used. The values of peak power of the installation, number of modules and the modules surface are presented in table 9 for the 1st day of the month from March to October 2012 at 1 pm. This power varies with time and evaporating temperature as shown in figure 12.

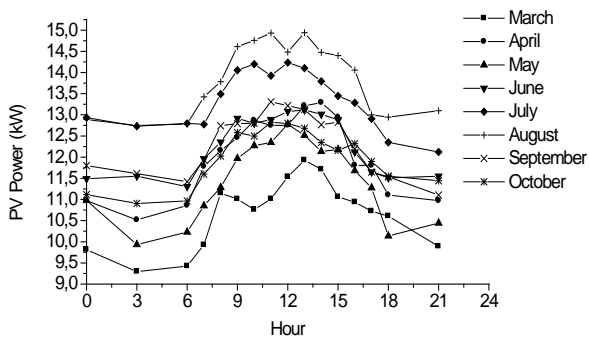


Figure 12: Hourly variation of PV power for the 1st days of the months from March to October 2012, for an evaporating temperature $T_e=0^\circ\text{C}$

According to the results, it is higher in August with a value of 14.94 kWp and insolation of 4.86 Wh/m²/day. The minimum value is obtained in March at 3 am with 9.29 kWp and the maximum at 2pm (14.94 kWp) on August, while on April there is a minimum value of 9.93 kWp at 3 pm and a maximum of 12.77 kWp.

Figure 13 gives the hourly variation of the output of the PV modules for evaporating temperatures of -10 °C, -5 °C, 0 °C, 5 °C and 10 °C in April. It could be seen that it is low for an evaporating temperature of 10 °C and higher for an evaporating temperature of -10 °C. We could therefore conclude that when the evaporating temperature decreases as the power of PV modules increases.

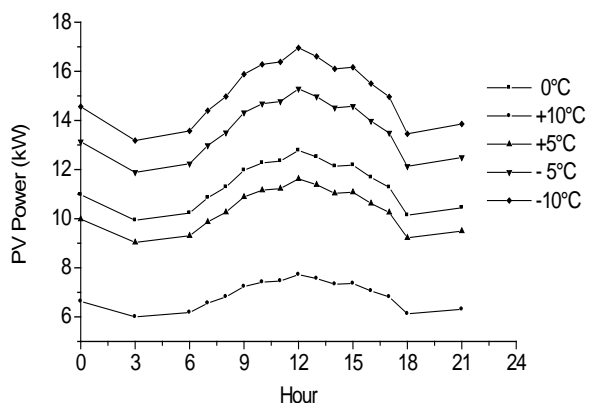


Figure 13: Hourly variation of PV power for evaporating temperatures of 0°C, +10°C, +5°C, -5°C and -10°C on 1st April 2012

After calculating the different powers and energies provided by the PV panels as shown on figures 14 and 15, we can make a comparison between them and the powers and energies absorbed by the compressor.

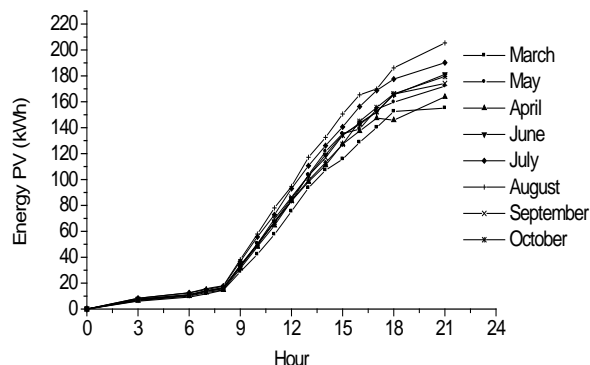


Figure 14: Hourly variation of PV energy for the 1st days of the months from March to October 2012, for an evaporating temperature $T_e= 0^\circ\text{C}$

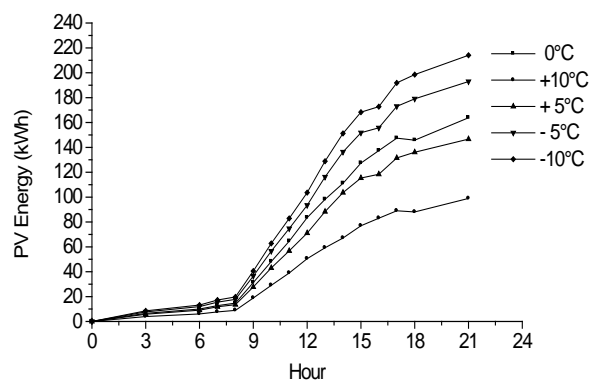


Figure 15: Hourly variation of PV energy for evaporating temperatures of 0°C, +10°C, +5°C, -5°C and -10°C on 1st April 2012

Figure 16 shows the evolution of the output of the PV panels and that absorbed by the compressor on April for an evaporating temperature of 0 °C. It could be seen that the energy provided by the PV panel is greater than that consumed by the compressor; it has a minimum value of 9.93 kW and a maximum value of 12.77 kW, while the power absorbed by the compressor varies from 4.8 to 6.18 kW.

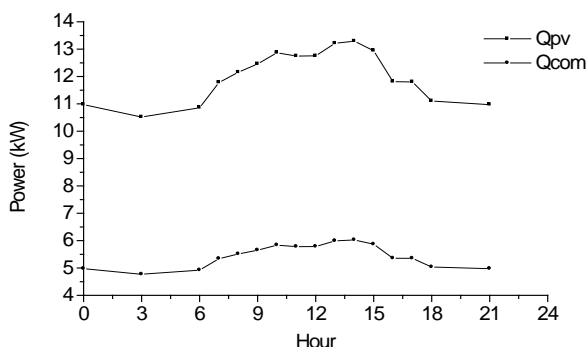


Figure 16: Comparison between the hourly power consumption of the compressor and the PV power generated on April 1st, 2012 for an evaporating temperature $T_e= 0^\circ\text{C}$

Figure 17 presents a comparison between the energy absorbed by the compressor and the energy of PV panels in April for an evaporating temperature of 0 °C. It could be

checked that, between 4 pm and 9 pm, energy exceeds consumption. So the excess energy could be stored in batteries for latter uses at operating hours of low energy such as 8 am, 9 am, 4 pm, 5 pm and 6 pm.

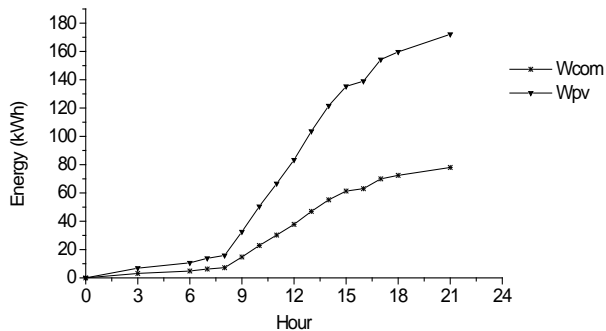


Figure 17: Comparison between hourly energy consumption of the compressor and the PV energy generated on April 1st, 2012 for an evaporating temperature $T_e = 0^\circ\text{C}$

4.6. Evaluation of the overall efficiency of the system

Considering the values of the total heat load and PV power calculated from March to October the overall monthly efficiencies of the system are presented in table 10. It could be seen that the overall performance of the plant also varies with season. In the warmer months, we have higher values. We can therefore conclude that, our SE-VCR system will have better returns for the months of March, April and May, with a maximum value of 35%.

5. Conclusions and Recommendations

The overall objective of this work was to contribute to the improvement of thermal comfort in living environments by using a cooling system coupled to a solar installation. An evaluation of the hourly cooling load was done by the means of heat balance due to walls, solar radiation, air renewal, occupants, lighting and electrical appliances. The variations of the various parameters were calculated as well as the minimum area of the photovoltaic panel to satisfy the power demand of the compressor. The results showed that the effective power of the compressor varies between 5.33 kW and 6 kW; the coefficient of refrigerating performance varies from 3.28 to 3.74 while the efficiency of the installation varies from 17 % to 35 %. Finally, the proposed SE-VCR system can successfully be operated in dry tropical areas to improve thermal comfort. The results obtained in this paper could be used in some other areas like Niamey in Niger; Ndjamena in Chad; Ouagadougou in Burkina Faso and other regions with same climatic characteristics. However, further investigations should be made to see the possibility of using adsorption refrigeration systems in the Sudano-Sahelian areas.

Acknowledgements

Authors are grateful to the Meteorological service of the airport of Maroua-Salak for providing them with data necessary to the realization of this work.

References

- [1] Maalouf Chadi (2006). Étude du potentiel de rafraîchissement d'un système évaporatif à désorption avec régénération solaire. PhD Thesis, Université de la Rochelle, France, 220P.
- [2] Noël Djongyang, René Tchinda and César Kapseu (2012) A Review of Solar Technologies For Buildings. African Journal of Science, Technology, Innovation and Development 4 (4): 11-36
- [3] César Kapseu, Noël Djongyang, George Elambo Nkeng, Maturin Petsoko, Daniel Ayuk Mbi Egbe (2012). Energies renouvelables en Afrique Subsaharienne, Harmattan, 370 p.
- [4] Mastrullo, R., Renno, C., (2010). A thermoeconomic model of a photovoltaic heat pump. Applied Thermal Engineering 30: 1959–1966.
- [5] Adnene Cherif, Ahmed Dhouib (2002). Dynamic modelling and simulation of a photovoltaic refrigeration plant. Renewable Energy 26: 143–153.
- [6] Mehmet Bilgili (2011). Hourly simulation and performance of solar electric vapor compression refrigeration system. Solar Energy 85: 1-12.
- [7] Fong, K.F., Chow Tai Tai, Lee, C.K., Lin, Z., Chan Lung Sang, (2010). Comparative study of different solar cooling systems for buildings in subtropical city. Solar Energy 84:227–244.
- [8] Todd Otanicar, Robert A. Taylor, Patrick E. Phelan (2012). Prospects for solar cooling-An economic and environmental assessment. Solar Energy 86 (5) 1287–1299.
- [9] Dai YJ, Wang RZ, Ni L (2003). Experimental investigation and analysis on a thermoelectric refrigerator driven by solar cells. Solar Energy Mater. Solar Cells, 77: 377-391.
- [10] Abdul-Wahab SA, Elkamel A, Al-Damkhi AM, Al-Habsi IA, Al-Rubai'ey' HS, Al-Battashi AK, Al-Tamimi AR, Al-Mamari KH, Chutani MU (2009). Design and experimental investigation of portable solar thermoelectric refrigerator. Renewable Energy, 34: 30-34.
- [11] Kaplanis S, Papanastasiou N (2006). The study and performance of a modified conventional refrigerator to serve as a PV powered one. Renewable Energy, 31: 771-780.
- [12] Dieng AO, Wang RZ (2001). Literature review on solar adsorption technologies for ice-making and air conditioning purposes and recent developments in solar technology. Renewable Sustain. Energy Rev., 5: 313-342.
- [13] Fan Y, Luo L, Souyri B (2007). Review of solar sorption refrigeration technologies: Development and applications. Renewable Sustain. Energy Rev., 11: 1758-1775.
- [14] S.M. Xu , X.D. Huang ,R.Du (2011) An investigation of the solar powered absorption refrigeration system with advanced energy storage technology. Solar Energy 85: 1794–1804.
- [15] [15] K.F. Fong, C.K. Lee, T.T. Chow, Z. Lin, L.S. Chan (2010). Solar hybrid air-conditioning system for high temperature cooling in subtropical city. Renewable Energy 35:2439- 2451

- [16] Axaopoulos PJ, Theodoridis MP (2009). Design and experimental performance of a PV Ice-maker without battery. *Solar Energy*, 83: 1360-1369.
- [17] Ewert MK, Agrella M, Frahm J, Bergeron DJ, Berchowit D (1998). Experimental evaluation of a solar PV-refrigerator with Thermoelectric, Stirling and Vapor Compression Heat Pumps. *Proceedings of Solar' 98*, ASES. http://solar.nmsu.edu/publications/pv_direct_refrig.pdf
- [18] Papadopoulos AM, Oxizidis S, Kyriakis N (2003). Perspectives of solar cooling in view of the developments in the air-conditioning sector. *Renewable Sustainable Energy Rev.*, 7: 419-438.
- [19] Sözen A, Özalp M (2005). Solar-driven ejector-absorption cooling system. *Appl. Energy*, 80: 97-113.
- [20] Desideri U, Proietti S, Sdringola P (2009). Solar-powered cooling systems: Technical and economic analysis on industrial refrigeration and air-conditioning applications. *Appl. Energy*, 86: 1376-1386.
- [21] C. Sanjuan, S. Soutullo, M.R. Heras (2010). Optimization of a solar cooling system with interior energy storage. *Solar Energy* 84: 1244–1254.
- [22] Anyanwu EE (2003). Review of solid adsorption solar refrigerator I: an overview of the refrigeration cycle. *Energy Conversion Manage.*, 44: 301-312.
- [23] Anyanwu EE (2004). Review of solid adsorption solar refrigeration II: An overview of the principles and theory. *Energy Conversion Manage.*, 45: 1279-1295.
- [24] Noël Djongyang, René Tchinda, Donatien Njomo (2012). Estimation of some comfort parameters for sleeping environments in dry-tropical sub-Saharan Africa region. *Energy Conversion and Management* 58:110-119.
- [25] Mehmet Azmi Aktacir (2011). Experimental study of a multi-purpose PV-refrigerator system. *International Journal of Physical Sciences Vol. 6(4)*, pp. 746-757
- [26] Noël Djongyang, René Tchinda (2010). An investigation into thermal comfort and residential thermal environments in the intertropical sub-Saharan Africa region: Field study report during the Harmattan season in Cameroon, *Energy Conversion and Management* 51: 1391-1397.
- [27] Belhadj Mohammed (2008). Modélisation d'un Système de Captage Photovoltaïque Autonome. Master Thesis, University of Bechar, Algeria.
- [28] Noël Jabbour (2011). Intégration des systèmes à absorption solaire de petites puissances aux bâtiments - approche multifonction solaire: chauffage, ECS et rafraîchissement. PhD Thesis, University of Lyon, 163 pages.
- [29] Butti K. and Perlin J (1981). *A Golden Thread (2500 Years of Solar Architecture and Technology)*. New York: Van Nostrand Reinhold.
- [30] Weiss W. Bergmann I. and Faninger G (2006). *Solar Heating Worldwide: Markets and Contribution to Energy Supply 2004*. Paris: International Energy Agency Solar Heating and Cooling Program.
- [31] Mamadou Adj (1987). Etude et réalisation d'un prototype de réfrigérateur solaire a réserve de froid destiné à la conservation des vaccins. PhD Thesis, Cheick Anta Diop University, Senegal, 136 Pages.
- [32] Weiss W.W (2003). *Solar Heating Systems for Houses - A Design Handbook for Solar Combisystems.s.l.:* Earthscan 9781902916460.
- [33] Jacques Bonnin, P.J. Wilbur and Susumu Karaki (1980). *Réfrigération solaire*, SCM Paris.
- [34] N. Medini, B. Marmottant, ES. Golliet Ph. Grenier (1991). Study of a solar icemaker Machine. *International Journal of Refrigeration* 14: 363-367.

Author Profile



Armand Noël Ngueche Chedop received a Msc Degree in Electronics, Electrotechnics and Automatics from the University of Ngaoundere and a Master of Engineering in Renewable Energies from the Higher Institute of The Sahel of the University of Maroua in 2012 and 2014, respectively. He is now preparing a PhD Degree in Energy Systems and the Environment at the University of Maroua in Cameroon.



Noël Djongyang received a PhD Degree in Energy systems from the University of Yaounde I in 2010. From 2007 to 2013, he was a senior lecturer at the Faculty of Science of the University of Ngaoundere. He is since 2013, the Head of Department of Renewable Energies at the Higher Institute of the Sahel of the University of Maroua in Cameroon.



Zaatri Abdelouahab graduated as an Electrical Engineer from the Université Catholique de Louvain-la-Neuve, Belgium in 1981. He got a Magister on Electronics from the Electronics Institute of the University of Constantine in 1993. He received a PhD Degree from the "Flamish University", Leuven, Belgium. He is now a full professor at the Faculty of Engineering Science of the University of Constantine 1 in Algeria.